ADVANCED SCIENCE Open Access
www.advancedscience.com

Ultra-Narrowband Blue Multi-Resonance Thermally Activated Delayed Fluorescence Materials

*Susumu Oda, Bungo Kawakami, Masaru Horiuchi, Yuki Yamasaki, Ryosuke Kawasumi, and Takuji Hatakeyama**

Ultra-narrowband blue multi-resonance-induced thermally activated delayed fluorescence (MR-TADF) materials (V-DABNA and V-DABNA-F), consisting of three DABNA subunits possessing phenyl or 2,6-difluorophenyl substituents on the peripheral nitrogen atoms are synthesized by one-shot triple borylation. Benefiting from the inductive effect of fluorine atoms, the emission maximum of V-DABNA-F (464 nm) is blueshifted from that of the parent V-DABNA (481 nm), while maintaining a small full width at half maximum (FWHM, 16 nm) and a high rate constant for reverse intersystem crossing (6.5 × 10^5 s^{-1}). The organic light-emitting diodes (OLEDs) using V-DABNA and V-DABNA-F as emitters are fabricated by vapor deposition and exhibit blue emission at 483 and 468 nm with small FWHMs of 17 and 15 nm, corresponding to Commission Internationale d'Éclairage coordinates of (0.09, 0.27) and (0.12, 0.10), respectively. Both devices achieve high external quantum efficiencies of 26.2% and 26.6% at the maximum with minimum efficiency roll-offs of 0.9% and 3.2%, respectively, even at 1000 cd m^{-2}, which are record-setting values for blue MR-TADF OLEDs.

1. Introduction

Organic light-emitting diodes (OLEDs) using thermally activated delayed fluorescence (TADF) emitters have offered high electroluminance efficiency without the use of precious metals by harvesting both singlet and triplet excitons through reverse intersystem crossing (RISC).[1,2] Conventional TADF materials include donor and acceptor groups, which separate the highest occupied molecular orbital (HOMO) and lowest unoccupied molecular orbitals (LUMO), reduce the singlet–triplet energy gap (ΔE_{ST}) and promote the RISC process. However, the D-A type TADF molecules exhibit broad emission due to the structural relaxation in the excited states and suffer from low color purity, which hinders their widespread practical application.

To overcome this drawback, we have developed TADF materials with a new molecular design based on the multi-resonance (MR) effects of boron and nitrogen atoms, which enable the alternate localization of HOMOs and LUMOs at different carbon atoms on the same benzene ring.[3] This unique HOMO–LUMO separation successfully suppressed not only the structural relaxation, but also the vibronic coupling between the S_1–S_0 transition and stretching/scissoring vibration to achieve both high photoluminescence quantum yield (PLQY) and high color purity. Inspired by our first report on the MR-TADF material (**DABNA**),[3b] intensive studies have been carried out on the structural modification,[3-7] revealing that π-extension is an effective way to improve color purity and enhance the RISC rate constant (k_{RISC}).[4] For example, we have reported an ultrapure deep-blue MR-TADF material (***ν*-DABNA**), exhibiting narrowband emission at 467 nm with a full width at half maximum (FWHM) of 18 nm and k_{RISC} of 2.0 × 10^5 s^{-1}.[3d] Subsequently, we have successfully synthesized BN-embedded expanded helicene (**V-DABNA-Mes**) by one-shot triple borylation.[3i] Benefiting from the large π-helical structure, **V-DABNA-Mes** exhibited ultra-narrowband blue MR-TADF with an extremely small FWHM of 16 nm and a high k_{RISC} of 4.4 × 10^5 s^{-1}. However, the large molecular weight of **V-DABNA-Mes**, owing to the mesityl groups, hampered the fabrication of an OLED device by vapor deposition. Herein, we report a synthesis of V-DABNA derivative (**V-DABNA**), which enabled the fabrication of a vacuum-deposited OLED device with improved OLED performance including external quantum efficiency (EQE) and operational lifetime. Furthermore, we synthesized a fluorine-substituted derivative (V-DABNA-F) to realize a hypsochromic shift of V-DABNA-derived sky-blue emission without losing color purity using the inductive effect of fluorine atoms[5] and

S. Oda, B. Kawakami, M. Horiuchi, Y. Yamasaki
Department of Chemistry
Graduate School of Science and Technology
Kwansei Gakuin University
2-1 Gakuen, Sanda, Hyogo 669-1337, Japan
M. Horiuchi, T. Hatakeyama
Department of Chemistry
Graduate School of Science
Kyoto University
Sakyo-ku, Kyoto 606-8502, Japan
E-mail: hatake@kuchem.kyoto-u.ac.jp
R. Kawasumi
SK JNC Japan Co., Ltd.
25-1 Goi Kaigan, Ichihara, Chiba 290-8551, Japan

The ORCID identification number(s) for the author(s) of this article can be found under https://doi.org/10.1002/advs.202205070

DOI: 10.1002/advs.202205070

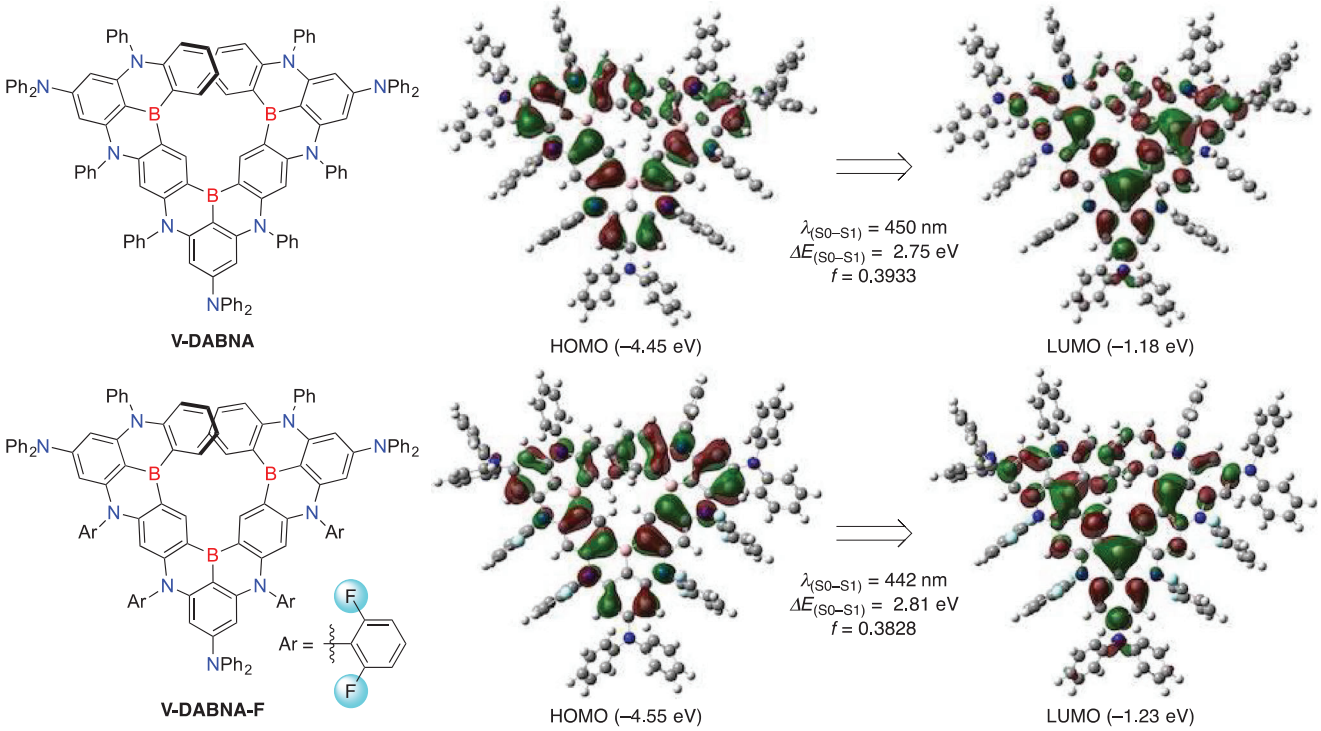

Figure 1. Chemical structures and Kohn–Sham frontier orbitals of **V-DABNA** and **V-DABNA-F** with the oscillator strength (f) and S_0–S_1 transition energies (ΔE, λ) at the B3LYP/6-31G(d) level of theory.

developed a highly efficient ultrapure deep-blue OLED device using it as an emitter.

2. Results and Discussion

According to the density functional theory (DFT) calculations at the B3LYP/6-31G(d) level of theory (**Figure 1**), both HOMO and LUMO energy levels of **V-DABNA-F** (−4.55 and −1.23 eV, respectively) are lower than those of **V-DABNA** (−4.45 and −1.18 eV, respectively). This is attributed to the inductive effect of fluorine atoms, which reduces the electron density of nitrogen atoms, resulting in a larger HOMO–LUMO energy gap. Thus, the S_0–S_1 transition energy of **V-DABNA-F** (2.81 eV) is larger than that of **V-DABNA** (2.75 eV), suggesting blueshifted emission.[6] Note that the transition energy of the 3,5-substituted derivative is 2.78 eV due to the weaker inductive effect (Figure S5, Supporting Information). Furthermore, time-dependent DFT calculations on **V-DABNA-core** and **V-DABNA-F-core** revealed a small ΔE_{ST} (39 and −9.5 meV) and large spin–orbit coupling matrix elements ($\langle S_1|\hat{H}_{SOC}|T_1\rangle$: 0.009 and 0.005 cm^{-1}, $\langle S_1|\hat{H}_{SOC}|T_2\rangle$: 0.084 and 0.091 cm^{-1}), suggesting a high k_{RISC} based on the relationship of k_{RISC} with $\langle S_n|\hat{H}_{SOC}|T_n\rangle$ and ΔE_{ST} ($k_{RISC} \propto \langle S_n|\hat{H}_{SOC}|T_n\rangle^2/\Delta E_{ST}$) (Figure S3, Supporting Information).[8]

Syntheses of **V-DABNA** and **V-DABNA-F** are shown in **Scheme 1**. The precursor **5** was prepared by Buchwald–Hartwig coupling in five steps from commercially available 1-bromo-3,5-dichlorobenzene. In the presence of BBr_3 (16 equiv), one-shot triple borylation of **5** occurred at 200 °C to afford **V-DABNA** in 11% yield. Moreover, this protocol was applied to fluorine-substituted precursor **5-F**, affording **V-DABNA-F** in 35% yield. The higher yield of **V-DABNA-F** is attributed to the 2,6-difluorophenyl groups, which suppressed the borylation at undesired reaction sites (Figure S4, Supporting Information).

The photophysical properties of **V-DABNA** and **V-DABNA-F** were measured in 1 wt%-doped poly(methyl methacrylate) (PMMA) films (**Figure 2** and **Table 1**). Notably, **V-DABNA** exhibited sky-blue emission at 481 nm with small FWHM of 17 nm and high PLQY of 90% (Figure 2a). The overlap of terminal phenyl ring may contribute to the larger redshift from ***ν*-DABNA** (467 nm) to **V-DABNA** (481 nm) than that from **DABNA-1** (460 nm) to ***ν*-DABNA** (467 nm).[3b,d] In addition, **V-DABNA-F** exhibited deep-blue emission at 464 nm, which was significantly blueshifted with respect to the parent **V-DABNA**, as predicted by time-dependent DFT calculations (Figure 2c). The small shoulder peaks around 510 and 495 nm in **V-DABNA** and **V-DABNA-F**, respectively, are attributed to the vibronic coupling between S_1–S_0 transition and stretching/scissoring vibration, which are mostly suppressed by the MR effect. The FWHM and PLQY of **V-DABNA-F** are 16 nm and 81%, respectively, which are similar to those of **V-DABNA**, indicating that the MR effect is maintained despite the incorporation of fluorine atoms. Based on the onset energies of fluorescence and phosphorescence, the ΔE_{ST} of 6.0 and 4.9 meV was determined for **V-DABNA** and **V-DABNA-F**, respectively. The transient decay curves of **V-DABNA** and **V-DABNA-F** showed two components with prompt lifetimes of 6.9 and 6.6 ns and delayed lifetimes of 1.9 and 1.7 µs, respectively (Figure 2b,d). Based on the obtained values of quantum yields and lifetimes, the rate constants of fluorescence (k_F), internal conversion (k_{IC}), intersystem crossing (k_{ISC}), and k_{RISC} were determined by Adachi's method (Figure 2b,d).[9] The k_{RISC} values

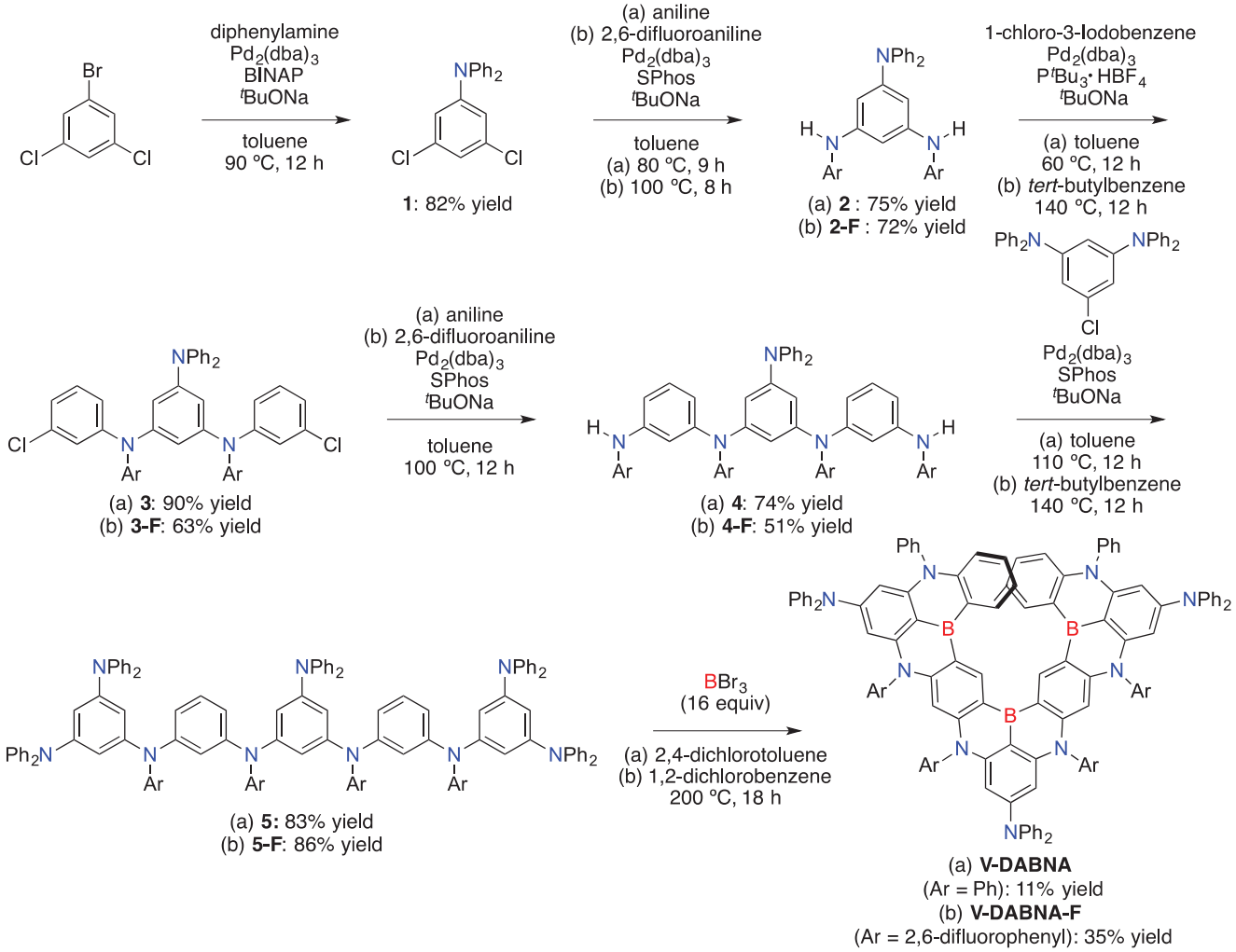

Scheme 1. Synthesis of a) **V-DABNA** and b) **V-DABNA-F**.

of **V-DABNA** and **V-DABNA-F** are 5.7×10^5 and 6.5×10^5 s^{-1}, respectively, which are higher than that of **V-DABNA-Mes** (4.4×10^5 s^{-1}) (Table 1). Although the k_F values are comparable between **V-DABNA** and **V-DABNA-F** (1.2×10^8 and 1.1×10^8 s^{-1}, respectively), the k_{IC} value of **V-DABNA-F** (2.7×10^7 s^{-1}) is larger than that of **V-DABNA** (1.3×10^7 s^{-1}), resulting in the lower PLQY in PMMA. The higher PLQY of 0.91 was observed for **V-DABNA-F** in toluene solution (Table S3, Supporting Information) suggests that aggregation in PMMA causes bimolecular quenching[10] or that the large dielectric constant of PMMA accelerates the IC process.

To demonstrate the potential of the proposed emitters, devices with the following structure were fabricated: indium tin oxide (ITO, 50 nm); *N,N′*-di(1-naphthyl)-*N,N′*-diphenyl-(1,1′-biphenyl)-4,4′-diamine (**NPD**, 40 nm); tris(4-carbazolyl-9-ylphenyl)amine (**TCTA**, 15 nm); 1,3-bis(*N*-carbazolyl)benzene (**mCP**, 15 nm); 1 wt% **V-DABNA** or **V-DABNA-F** emitter and 99 wt% **DOBNA-Tol**[3g] (20 nm); 3,4-di(9H-carbazol-9-yl)benzonitrile (**3,4-2CzBN**,[11a] 10 nm); 2,7-bis(2,2′-bipyridine-5-yl)triphenylene (**BPy-TP2**,[11b] 20 nm); LiF (1 nm); and Al (100 nm). The electroluminescence characteristics, ionization potentials, and electron affinities of the fabricated devices are shown in **Figure 3**. The **V-DABNA**-based device exhibited ultra-narrowband blue emission at 483 nm with an FWHM of 17 nm (92 meV) and corresponding Commission Internationale d'Éclairage (CIE) coordinates of (0.09, 0.27). Notably, the fabricated device achieved excellent EQE of 26.2%, 26.2%, and 25.3% at 1, 100, and 1000 cd m^{-2}, respectively, with the minimum efficiency roll-off of 0.1% and 0.9% at 100 and 1000 cd m^{-2}, respectively. These characteristics were significantly improved compared to the previously reported, solution-processed OLED device employing **V-DABNA-Mes** as an emitter and are record-setting for blue MR-TADF materials (Table S5, Supporting Information). Thus, the decrease in molecular weight by replacing mesityl groups with phenyl groups enabled the fabrication of vacuum-deposited OLED device, which improved the carrier balance and suppressed the efficiency-roll off. The half-lifetime (LT_{50}) of the **V-DABNA**-based device was 184 h with an initial luminance of 500 cd m^{-2}, which is longer than that of ***ν*-DABNA** (2 h with an initial luminance at 500 cd m^{-2})[12] due to the high k_{RISC} (Figure S10, Supporting Information). Furthermore, the **V-DABNA-F**-based device exhibited ultrapure deep-blue emission

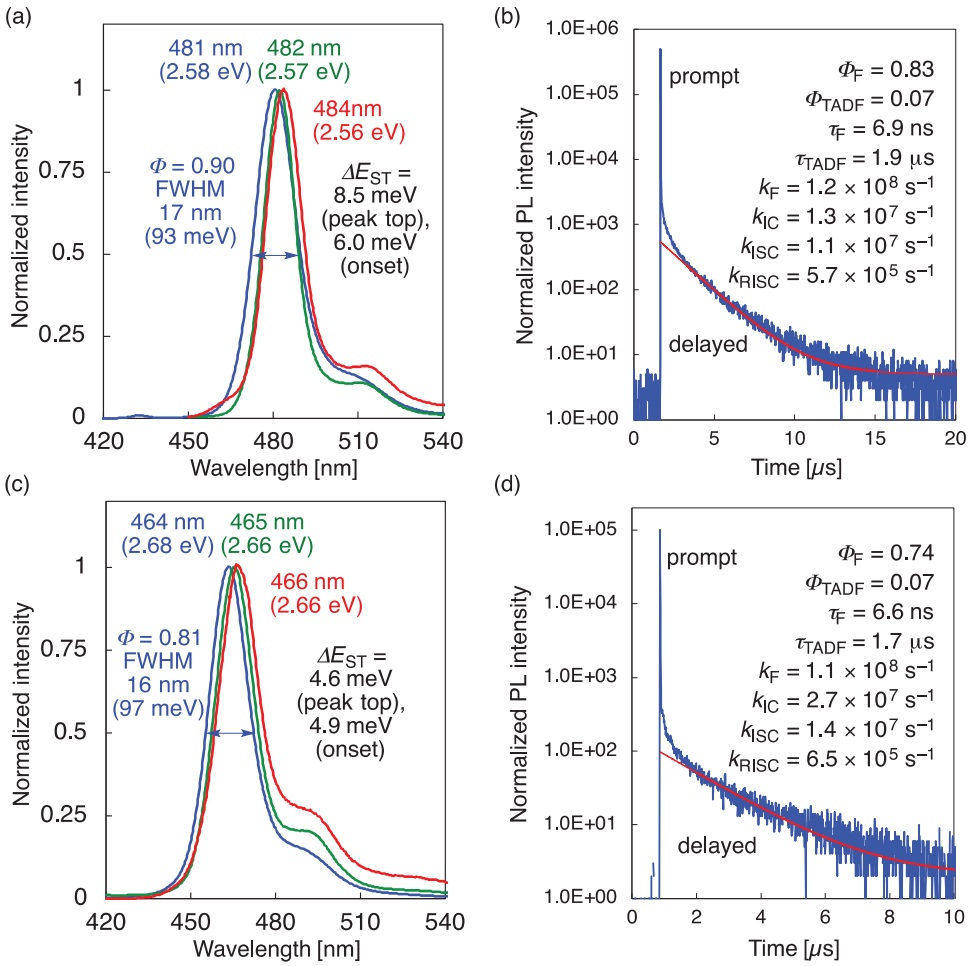

Figure 2. Photophysical properties of **V-DABNA** and **V-DABNA-F** in poly(methyl methacrylate) (PMMA) (1 wt%-doped films). Fluorescence spectra of a) **V-DABNA** and c) **V-DABNA-F** at 300 K (blue) and at 77 K with (red)/without (green) a delay time of 25 ms. Transient PL decay curves for b) **V-DABNA** and d) **V-DABNA-F**. The red curves represent the single exponential fitting data [background = (b) 5, (d) 2].

Table 1. Photophysical properties of **V-DABNA** and **V-DABNA-F** in poly(methyl methacrylate) (PMMA) (1 wt%-doped films).

Compound	Φ[a]	Φ_F[b]	Φ_{TADF}[b]	τ_F[c] [ns]	τ_{TADF}[c] [μs]	k_F[d] × 10^8 [s^{-1}]	k_{IC}[d] × 10^7 [s^{-1}]	k_{ISC}[d] × 10^7 [s^{-1}]	k_{RISC}[d] × 10^5 [s^{-1}]
V-DABNA	0.90	0.83	0.07	6.9	1.9	1.2	1.3	1.1	5.7
V-DABNA-F	0.81	0.74	0.07	6.6	1.7	1.1	2.7	1.4	6.5
V-DABNA-Mes	0.80	0.76	0.04	7.0	2.4	1.1	2.7	0.73	4.4

[a] Absolute photoluminescence quantum yield [b] Fluorescent and TADF components determined from the total Φ and contribution of the integrated area of each component in the transient spectra to the total integrated area [c] Lifetimes calculated from fluorescence decay [d] Decay rates of fluorescence (k_F), internal conversion from S_1 to S_0 (k_{IC}), intersystem crossing from S_1 to T_1 (k_{ISC}), and reverse intersystem crossing from T_1 to S_1 (k_{RISC}) were calculated from Φ, Φ_F, Φ_{TADF}, τ_F, and τ_{TADF} according to Adachi's method.

at 468 nm with an FWHM of 15 nm (87 meV), which is the smallest value for the reported blue MR-TADF materials (Table S5, Supporting Information). The corresponding CIE coordinates are (0.12, 0.10), and the EQEs are 26.6%, 25.8%, and 23.4% at 1, 100, and 1000 cd m^{-2}, respectively. The LT_{50} of the **V-DABNA-F**-based device was 3.6 h with an initial luminance of 500 cd m^{-2}, which is longer than that of ***ν*-DABNA** but shorter than that of **V-DABNA**. This is attributed to the electron trap caused by the larger electron affinity of **V-DABNA-F** (2.58 eV vs 2.53 eV, Figure 3a), which resulted in the C–N bond cleavage. Thus, the device lifetime can be improved by enhancing the electron affinity of host materials. In order to gain insight into high EQE, the angle dependence of the photoluminescence using codeposition films in **DOBNA-Tol** were measured (Figure S11, Supporting Information). Notably, the orientational order parameters (S) of **V-DABNA** and **V-DABNA-F** were determined to be −0.426 and −0.423, respectively, which are closer to the theoretical value (S = −0.5) for a perfectly horizontal orientation than that

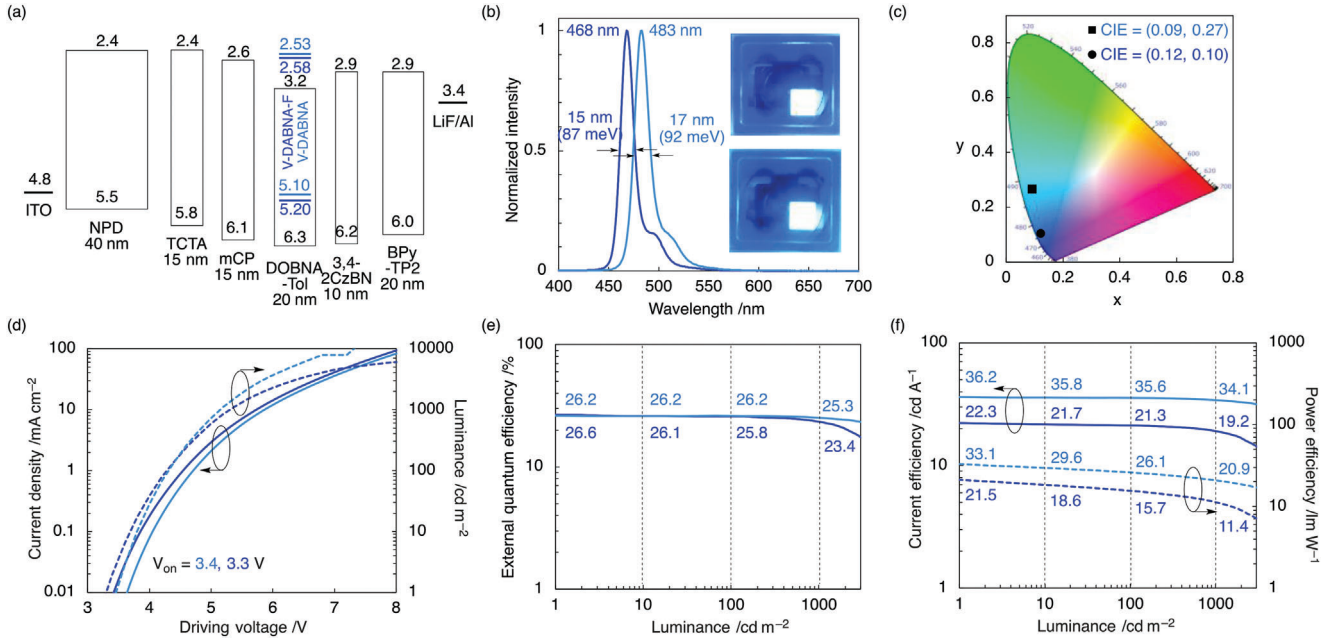

Figure 3. Characteristics of fabricated OLED devices using **V-DABNA** (sky-blue) and **V-DABNA-F** (blue) as emitters. a) Device structure, ionization potentials (I_p), and electron affinities (E_a) (in eV) for each component. The I_p and E_a of **V-DABNA** and **V-DABNA-F** were estimated from those of **V-DABNA-Mes** and their HOMO/LUMO energy levels. b) Normalized EL spectra of the devices in operation. Inset: electroluminescence of the device. c) Commission Internationale d'Éclairage (CIE) (x,y) coordinates. d) Current density (solid) and luminance (dashed) versus driving voltage. e) External quantum efficiency (EQE) versus luminance. f) Current efficiency (solid) and power efficiency (dashed) versus luminance.

of ***ν*-DABNA** ($S = -0.407$), resulting in high light outcoupling efficiency.

3. Conclusion

We synthesized ultra-narrowband blue MR-TADF materials (**V-DABNA**, **V-DABNA-F**) by one-shot triple borylation. The inductive effect of fluorine atoms effectively lowered the HOMO energy of **V-DABNA**, which led to an increase in energy of the HOMO–LUMO gap. As a result, **V-DABNA-F** exhibited ultrapure deep-blue TADF with a small FWHM of 16 nm, which is blueshifted from parent **V-DABNA**. The OLED fabricated by vapor deposition using **V-DABNA** as an emitter exhibited ultra-narrowband blue emission at 483 nm with an FWHM of 17 nm, and achieved an excellent maximum EQE of 26.2%, with minimum efficiency roll-offs of 0.1% and 0.9% at 100 and 1000 cd m^{-2}, respectively, which are record-setting values for blue MR-TADF materials. In addition, the OLED fabricated using **V-DABNA-F** exhibited ultrapure deep-blue emission at 468 nm with an FWHM of 15 nm, which is narrowest among the reported blue MR-TADF materials. Thus, we have established a successful approach for the fabrication of ultra-narrowband blue MR-TADF emitters, which will pave the way for the development of highly efficient blue OLEDs.

Supporting Information

Supporting Information is available from the Wiley Online Library or from the author.

Acknowledgements

This work was supported by a Grant-in-Aid for Transformative Research Areas (A) "Condensed Conjugation" (JSPS KAKENHI Grant Number JP20H05862 and JP20H05863) from MEXT, Japan. T.H. acknowledges the Asahi Glass Foundation for financial support. The authors are grateful to Mr. Hiroyuki Tanaka (SK JNC Japan Co., Ltd.), Dr. Masakazu Kondo and Dr. Takeshi Matsushita (JNC Co.) for their experimental support and valuable inputs.

Conflict of Interest

The authors declare no conflict of interest.

Data Availability Statement

The data that support the findings of this study are available in the supplementary material of this article.

Keywords

fluorine, multi-resonance effect, narrowband emission, organic light-emitting diodes, thermally activated delayed fluorescence

Received: September 3, 2022
Revised: October 13, 2022
Published online: November 17, 2022

[1] a) H. Uoyama, K. Goushi, K. Shizu, H. Nomura, C. Adachi, *Nature* **2012**, *492*, 234; b) Q. Zhang, J. Li, K. Shizu, S. Huang, S. Hirata, H.

Miyazaki, C. Adachi, *J. Am. Chem. Soc.* **2012**, *134*, 14706; c) K. Goushi, K. Yoshida, K. Sato, C. Adachi, *Nat. Photonics* **2012**, *6*, 253.

[2] Reviews: a) M. Godumala, S. Choi, M. J. Cho, D. H. Choi, *J. Mater. Chem. C* **2016**, *4*, 11355; b) Y. Im, M. Kim, Y. J. Cho, J.-A. Seo, K. S. Yook, J. Y. Lee, *Chem. Mater.* **2017**, *29*, 1946; c) Z. Yang, Z. Mao, Z. Xie, Y. Zhang, S. Liu, J. Zhao, J. Xu, Z. Chi, M. P. Aldred, *Chem. Soc. Rev.* **2017**, *46*, 915; d) M. Y. Wong, E. Zysman-Colman, *Adv. Mater.* **2017**, *29*, 1605444; e) X. Cai, S.-J. Su, *Adv. Funct. Mater.* **2018**, *28*, 1802558; f) M. Godumala, S. Choi, M. J. Cho, D. H. Choi, *J. Mater. Chem. C* **2019**, *7*, 2172; g) H. Nakanotani, Y. Tsuchiya, C. Adachi, *Chem. Lett.* **2021**, *50*, 938.

[3] a) H. Hirai, K. Nakajima, S. Nakatsuka, K. Shiren, J. Ni, S. Nomura, T. Ikuta, T. Hatakeyama, *Angew. Chem., Int. Ed.* **2015**, *54*, 13581; b) T. Hatakeyama, K. Shiren, K. Nakajima, S. Nomura, S. Nakatsuka, K. Kinoshita, J. Ni, Y. Ono, T. Ikuta, *Adv. Mater.* **2016**, *28*, 2777; c) K. Matsui, S. Oda, K. Yoshiura, K. Nakajima, N. Yasuda, T. Hatakeyama, *J. Am. Chem. Soc.* **2018**, *140*, 1195; d) Y. Kondo, K. Yoshiura, S. Kitera, H. Nishi, S. Oda, H. Gotoh, Y. Sasada, M. Yanai, T. Hatakeyama, *Nat. Photonics* **2019**, *13*, 678; e) S. Oda, B. Kawakami, R. Kawasumi, R. Okita, T. Hatakeyama, *Org. Lett.* **2019**, *21*, 9311; f) N. Ikeda, S. Oda, R. Matsumoto, M. Yoshioka, D. Fukushima, K. Yoshiura, N. Yasuda, T. Hatakeyama, *Adv. Mater.* **2020**, *32*, 2004072; g) S. Oda, W. Kumano, T. Hama, R. Kawasumi, K. Yoshiura, T. Hatakeyama, *Angew. Chem., Int. Ed.* **2021**, *60*, 2882; h) H. Tanaka, S. Oda, G. Ricci, H. Gotoh, K. Tabata, R. Kawasumi, D. Beljonne, Y. Olivier, T. Hatakeyama, *Angew. Chem., Int. Ed.* **2021**, *60*, 17910; i) S. Oda, B. Kawakami, Y. Yamasaki, R. Matsumoto, M. Yoshioka, D. Fukushima, S. Nakatsuka, T. Hatakeyama, *J. Am. Chem. Soc.* **2022**, *144*, 106; j) S. Oda, T. Sugitani, H. Tanaka, K. Tabata, R. Kawasumi, T. Hatakeyama, *Adv. Mater.* **2022**, *34*, 2201778.

[4] a) X. Liang, Z.-P. Yan, H.-B. Han, Z.-G. Wu, Y.-X. Zheng, H. Meng, J.-L. Zuo, W. Huang, *Angew. Chem., Int. Ed.* **2018**, *57*, 11316; b) T. Northey, T. J. Penfold, *Org. Electron.* **2018**, *59*, 45; c) A. Pershin, D. Hall, V. Lemaur, J.-C. Sancho-Garcia, L. Muccioli, E. Zysman-Colman, D. Beljonne, Y. Olivier, *Nat. Commun.* **2019**, *10*, 597; d) Y. Zhang, D. Zhang, J. Wei, Z. Liu, Y. Lu, L. Duan, *Angew. Chem., Int. Ed.* **2019**, *58*, 16912; e) S. H. Han, J. H. Jeong, J. W. Yoob, J. Y. Lee, *J. Mater. Chem. C* **2019**, *7*, 3082; f) Y. Xu, C. Li, Z. Li, Q. Wang, X. Cai, J. Wei, Y. Wang, *Angew. Chem., Int. Ed.* **2020**, *59*, 17442; g) Y. Zhang, D. Zhang, J. Wei, X. Hong, Y. Lu, D. Hu, G. Li, Z. Liu, Y. Chen, L. Duan, *Angew. Chem., Int. Ed.* **2020**, *59*, 17499; h) S. M. Suresh, E. Duda, D. Hall, Z. Yao, S. Bagnich, A. M. Z. Slawin, H. Bassler, D. Beljonne, M. Buck, Y. Olivier, A. Köhler, E. Zysman-Colman, *J. Am. Chem. Soc.* **2020**, *142*, 6588; i) M. Yang, I. S. Park, T. Yasuda, *J. Am. Chem. Soc.* **2020**, *142*, 19468; j) M. Nagata, H. Min, E. Watanabe, H. Fukumoto, Y. Mizuhata, N. Tokitoh, T. Agou, T. Yasuda, *Angew. Chem., Int. Ed.* **2021**, *60*, 20280; k) Y. Zhang, D. Zhang, T. Huang, A. J. Gillett, Y. Liu, D. Hu, L. Cui, Z. Bin, G. Li, J. Wei, L. Duan, *Angew. Chem., Int. Ed.* **2021**, *60*, 20498; l) H. Lim, S.-J. Woo, Y. H. Ha, Y.-H. Kim, J.-J. Kim, *Adv. Mater.* **2022**, *34*, 2100161; m) P. Jiang, J. Miao, X. Cao, H. Xia, K. Pan, T. Hua, X. Lv, Z. Huang, Y. Zou, C. Yang, *Adv. Mater.* **2022**, *34*, 2106954; n) G. Liu, H. Sasabe, K. Kumada, H. Arai, J. Kido, *Chem. - Eur. J.* **2022**, *28*, e202201605; o) Y. Liu, X. Xiao, Z. Huang, D. Yang, D. Ma, J. Liu, B. Lei, Z. Bin, J. You, *Angew. Chem., Int. Ed.* **2022**, *61*, e202210210.

[5] Fluorine-substitution in ***ν*-DABNA**: a) T. Hatakeyama, K. Shiren, H. Tanaka, G. Wang, D. Baba, Y. Sasada, *WO2019198698 A1*, **2019**; b) K. R. Naveen, H. Lee, R. Braveenth, K. J. Yang, S. J. Hwang, J. H. Kwon, *Chem. Eng. J.* **2022**, *432*, 134381.

[6] Recent examples of blue MR-TADF materials: a) I. S. Park, M. Yang, H. Shibata, N. Amanokura, T. Yasuda, *Adv. Mater.* **2022**, *34*, 2107951; b) X. Lv, J. Miao, M. Liu, Q. Peng, C. Zhong, Y. Hu, X. Cao, H. Wu, Y. Yang, C. Zhou, J. Ma, Y. Zou, C. Yang, *Angew. Chem., Int. Ed.* **2022**, *61*, e202201588; c) J. Bian, S. Chen, L. Qiu, R. Tian, Y. Man, Y. Wang, S. Chen, J. Zhang, C. Duan, C. Han, H. Xu, *Adv. Mater.* **2022**, *34*, 2110547.

[7] Reviews: a) S. M. Suresh, D. Hall, D. Beljonne, Y. Olivier, E. Zysman-Colman, *Adv. Funct. Mater.* **2020**, *30*, 1908677; b) J.-M. Teng, Y.-F. Wang, C.-F. Chen, *J. Mater. Chem. C* **2020**, *8*, 11340; c) S. Oda, T. Hatakeyama, *Bull. Chem. Soc. Jpn.* **2021**, *94*, 950.

[8] a) J. Gibson, A. P. Monkman, T. J. Penfold, *ChemPhysChem* **2016**, *17*, 2956; b) M. K. Etherington, J. Gibson, H. F. Higginbotham, T. J. Penfold, A. P. Monkman, *Nat. Commun.* **2016**, *7*, 13680; c) P.-K. Samanta, D. Kim, V. Coropceanu, J.-J. Brédas, *J. Am. Chem. Soc.* **2017**, *139*, 4042; d) N. Aizawa, Y. Harabuchi, S. Maeda, Y.-J. Pu, *Nat. Commun.* **2020**, *11*, 3909; e) I. Kim, K. H. Cho, S. O. Jeon, W.-J. Son, D. Kim, Y. M. Rhee, I. Jang, H. Choi, D. S. Kim, *JACS Au* **2021**, *1*, 987; f) X. Wu, B.-K. Su, D.-G. Chen, D. Liu, C.-C. Wu, Z.-X. Huang, T.-C. Lin, C.-H. Wu, M. Zhu, E. Y. Li, W.-Y. Hung, W. Zhu, P.-T. Chou, *Nat. Photonics* **2021**, *15*, 780.

[9] a) Q. Zhang, H. Kuwabara, W. J. Potscavage, Jr., S. Huang, Y. Hatae, T. Shibata, C. Adachi, *J. Am. Chem. Soc.* **2014**, *136*, 18070; b) H. Kaji, H. Suzuki, T. Fukushima, K. Shizu, K. Katsuaki, S. Kubo, T. Komino, H. Oiwa, F. Suzuki, A. Wakamiya, Y. Murata, C. Adachi, *Nat. Commun.* **2015**, *6*, 8476.

[10] K. Stavrou, A. Danos, T. Hama, T. Hatakeyama, A. Monkman, *ACS Appl. Mater. Interfaces* **2021**, *13*, 8643.

[11] a) K. Togashi, S. Nomura, N. Yokoyama, T. Yasuda, C. Adachi, *J. Mater. Chem.* **2012**, *22*, 20689; b) Y. Tanaka, T. Takahashi, J. Nishide, Y. Hiraga, H. Nakanotani, C. Adachi, *Thin Solid Films* **2016**, *619*, 120.

[12] C.-Y. Chan, M. Tanaka, Y.-T. Lee, Y.-W. Wong, H. Nakanotani, T. Hatakeyama, C. Adachi, *Nat. Photonics* **2021**, *15*, 203.

